Fatigue Response of Bridge Deck Link Slabs Designed with Ductile Engineered Cementitious Composite (ECC)

Yun Yong Kim[1] and Victor C. Li[2]
[1] Department of Civil and Environmental Engineering, Korea Advanced Institute of Science and Technology, Daejeon, Korea
[2] Department of Civil and Environmental Engineering, University of Michigan, Ann Arbor, MI, USA

Abstract
Link slabs designed for macroscopically crack free concrete bridge decks system were experimentally tested. The property requirements of the link slab material were considered. Special focus was placed on the fatigue and durability performance. Introduction of a ductile Engineered Cementitious Composite (ECC) material is proposed for its ability to control crack width and to exhibit high ductile behavior, which are main performance requirements in the link slab. Experimental results of cyclic tests of full-scale ECC link slabs are compared with those of an ordinary reinforced concrete link slab. The fatigue response will be discussed with particular emphasis on the development of crack widths, which is important for durability against steel reinforcement corrosion. The significant enhancement of crack width control in ECC link slab suggest that the use of ECC material can be effective in extending the service life of repaired bridge decks system.

1. Introduction

Many highway bridges are composed of multiple span steel or prestressed concrete girders simply supported at piers or bents. The girders support cast-in-place concrete decks. A mechanical joint is typically employed at the end of the simple span deck to allow deck deformations imposed by girder deflection, concrete shrinkage, and temperature variations. It is well known that bridge deck joints are expensive to install and maintain. Deterioration of joint functionality due to debris accumulation can lead to severe damage in the bridge deck and substructure. The durability of beam ends, girder bearings, and supporting structures can be compromised by water leakage and flow of deicing chemicals through the joints. A possible approach to alleviate this problem is the elimination of mechanical deck joints in multispan bridges.

The section of the deck connecting the two adjacent simple-span girders is called the link slab. These systems have to focus on reducing or eliminating cracking in the concrete

deck rather than providing girder continuity. Caner and Zia[1] experimentally analyzed the performance of jointless bridge decks and proposed design methods for the link slab. These investigations revealed that the link slab was subjected to bending under typical traffic conditions rather than axial elongation. Tensile cracks were observed at the top of the link slab under service conditions due to a negative bending moment. For steel girders, the measured maximum crack width was 300μm at 40% of ultimate load and 750μm at 67% of ultimate load. They pointed out that additional tensile stress may be imposed on the link slabs due to shrinkage, creep, and temperature loading, and that crack width must be carefully controlled. The recommendation was to use epoxy coated reinforcing bars in the link slab in order to avoid reinforcement corrosion. To reduce the stiffness of the link slab, debonding of the link slab over the girder joint for a length equal to 5% of each girder span was also recommended.

The basis of the present suggested approach for the design of maintenance-free link slabs is an Engineered Cementitious Composite (ECC) with high ductile, strain-hardening deformation behavior in tension analogous to that of metals. In ECC, crack widths are an intrinsic material property governed by micromechanical parameters and typically limited to 60 to 80μm, which significantly reduces the penetration and leakage of water and corrosive substances.

The purpose of this paper is to demonstrate the performance of link slabs designed with ductile ECC material for macroscopically crack free concrete bridge decks. In the selection of ECC material, the property requirements of the link slab material were considered. The performance of ECC link slabs was evaluated by testing full-scale sections of link slab specimens. The fatigue cracking resistance, and design of link slab associated with the evolution of crack width, will be discussed.

2. Property requirements of link slab materials and ECC properties

For material selection, property requirements of ECC material for link slabs were examined prior to material design. As a minimum compressive strength, 35 MPa was adopted on the basis of widely chosen design compressive strength (27.5 MPa) of concrete in bridge deck slabs. Current AASHTO Standard Specifications for Highway Bridges 2002 (AASHTO code hereafter) provide maximum permissible crack width of 330μm in reinforced concrete (R/C) bridge deck in severe exposure condition. The influence of reduced crack width on the permeability of water contaminated by harmful substances such as chlorides introduced by deicing salt can be evaluated using reference data [2]. The data in Fig.1 indicate that for crack widths below 100μm the permeability coefficient remains relatively small and constant (10^{-10}m/s). At increasing crack widths, however, the permeability coefficient increases rapidly and reaches values several magnitudes higher (10^{-6}m/s at 330μm crack width). Therefore, the desired crack width was minimized to less than 100 μm to approach transport properties of sound concrete without macroscopic cracks for corrosion resistance.

Assuming 5% debond length between deck and girder, at each end of a bridge span of length, the strain capacity of ECC link slab demanded to accommodate the movement imposed by ΔT=50°C temperature variations and shrinkage strain (~0.1%)[3] and the maximum tensile strain (< 0.1%)[4] in the link slab due to the imposed bending moment. With a safety factor of two, the minimum required tensile strain capacity of ECC material was estimated to be 1.4% for link slab applications.

The ECC material used for link slab specimens utilized 2% by volume of PVA fibers tailored based on micromechanical principles[5], Type 1 ordinary Portland cement, fine aggregates, Type F fly ash, water, and a water-reducing admixture. The mix proportion of the ECC employed in this study is given in Table 1. Material properties obtained from this composition at the age of 28 days were a first crack strength of 4.0MPa at approximately 0.02% strain and an ultimate tensile strength of 6.0MPa at 3.7% strain (Fig.2). The averaged crack width for this ECC at peak load remains at 40 μm. The tensile strain hardening behavior and multiple cracking with crack widths below 100μm indicated the performance level of ECC. The compressive strength of ECC was 80MPa at 28 days and significantly higher than anticipated (35MPa). This indicates that the hardened properties of the ECC can meet and exceed the structural requirements of link slabs. Especially, the expected maximum imposed strain (1.4% with safety factor of two) is in the early strain-hardening regime of this ECC with micro crack width maintained below 100μm. These ECC properties will provide link slabs with significantly enhanced rotational and axial deformation capacity while controlling crack width, resulting in low permeability and reduced maintenance needs of jointless bridge deck systems with ECC link slabs.

Table 1. Mix proportion of the ECC employed in this study.

Cement	Water	Sand	Fly Ash	Superplasticizer	V_f
1.00	0.53	0.80	1.20	0.03	0.02

All numbers are weight ratios except for V_f(fiber volume fraction).

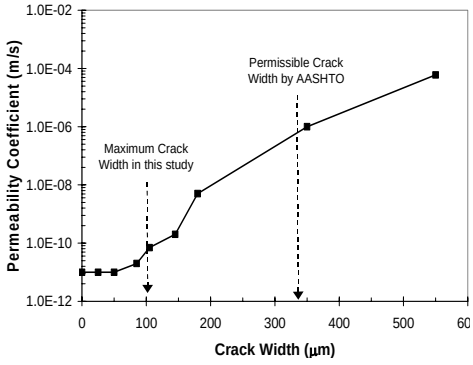

Fig.1 Permeability coefficient as a function of crack width [2].

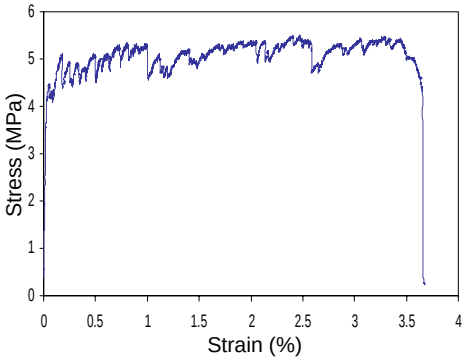

Fig.2 Typical tensile stress-strain behavior of the ECC designed for link slabs.

3. Experimental program

3.1 Testing configuration

While previous laboratory investigation of link slabs[1,4] involved testing of a 1/6 scaled bridge including a link slab with two adjacent spans, the present study focused on testing of a full-scale link slab portion exclusively. Therefore, the end rotations imposed on the link slab by the adjacent spans in a bridge were replicated in the laboratory.

The deformed shape and moment distribution due to applied load of a two-span bridge structure are schematically shown in Fig.3(a). Flexural crack formation was expected at the top of the link slab as illustrated in Fig.3(b). Therefore, the link slab specimens were designed to include the link slab within the distance between the points of inflection in the adjacent spans. The location of inflection point should be determined by the stiffness of the link slab. In case of zero stiffness, the point of inflection is located at the support, while for a continuous girder and deck its location is at 20% of the span length from the support. In the case of a link slab with girder discontinuity, the point of inflection is located within these boundaries.

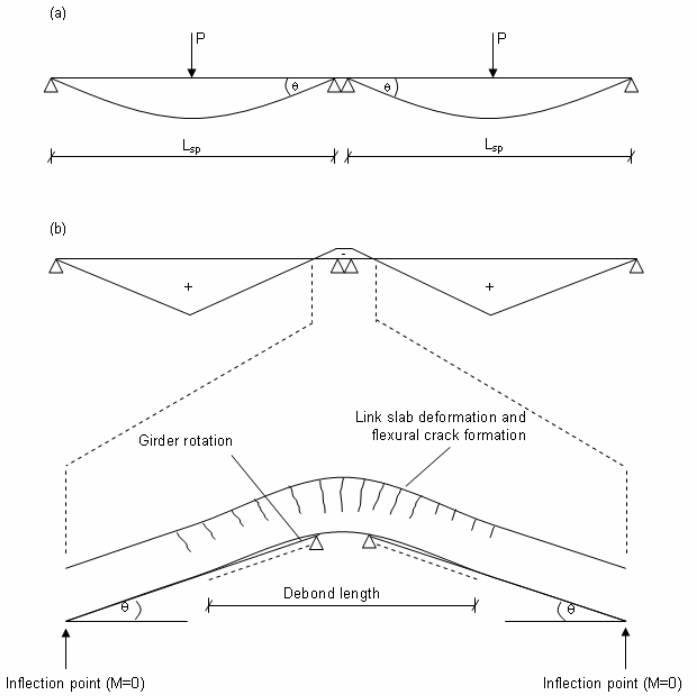

Fig.3 Schematics of two span bridge subjected to point load at midspan for (a) deformed shape of bridges; and (b) moment distribution on bridge span and corresponding deformed shape of link slab region

3.2 Design of test specimen

Fig.4 shows the specimen geometry of concrete and ECC link slabs, including the debond zone length (1.27m) equal to roughly 2.5% of each adjacent span. It is noted that the length and height dimensions of specimens are identical to a link slab between two adjacent 25m span bridges. The thickness of the link slab was 230mm, which corresponds to typical deck slabs in simply supported composite girder bridges. As described earlier, the location of inflection point should be located in the range from 0% up to 20% of the span. We employed an inflection point at 7% of the span based on a numerical analysis procedure.

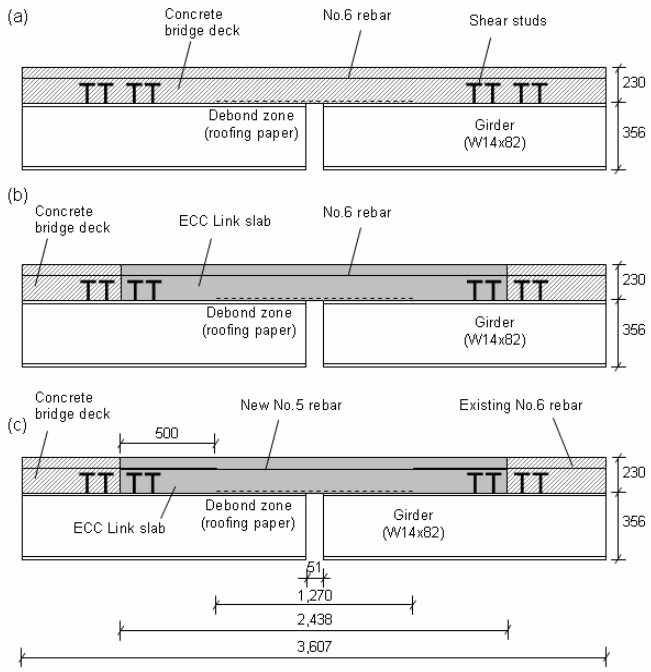

Fig.4 Geometry of link slab specimens for (a) LS-1; (a) LS-2; and (b) LS-3. (Dimensions shown are in mm)

Specimen LS-1, in which a concrete link slab reinforced with continuous No.6 reinforcing bars and adjacent spans were cast together, was used to simulate the concrete link slab new construction. According to the current limit stress criterion of R/C link slabs, the reinforcement ratio of the concrete link slab was determined to satisfy the stress criterion ($\sigma_s < 0.40\sigma_y$) at 0.0015 rad. end rotation angle. This is the expected rotation angle as derived by Caner and Zia [1]. The moment $M_{a,g}$ developed in the uncracked concrete link slab is a function of the elastic modulus of concrete E_c and geometrical dimensions. It is proportional to the imposed end rotation angle θ.

$$M_{a,g} = \frac{2E_C I_{ls,g}}{L_{ls}}\theta \qquad (1)$$

where $I_{ls,g}$ is the second moment of inertia of link slab based on uncracked section and L_{ls} is the debond length. In the debond zone, no shear connectors were used and 15-lb roofing paper was placed at the top of flange of the W14x82 girder.

Specimen LS-2 was prepared by removing the concrete from the link slab portion of specimen LS-1 and replacing it with an ECC link slab. This specimen was used to simulate the replacement of an R/C link slab with a new ECC link slab since the continuous reinforcement remained. The length of the link slab was 2.44m including 1.27m length of debond zone. The debond zone in the conventional concrete link slab has been designed to begin at the interface between deck slab and link slab, which results in locating the interface at the weakest part of the bridge deck system. In the present study, four shear studs were welded on the top of the girder flange (Fig.4(b)) in order to strengthen the interface between ECC link slab and R/C bridge deck.

In order to investigate the effects of the reinforcement ratio on fatigue performance of ECC link slab, a third specimen LS-3 was prepared. Specifically the focus of this test was on the fatigue performance of ECC link slab reinforced with a smaller amount of reinforcement compared to the design value and the fatigue cracking resistance of interface reinforced with the lap spliced existing rebar. This specimen was prepared by removing the ECC from the link slab portion of specimen LS-2 and pouring new ECC into the removed portion. The existing No.6 reinforcements were cut out with 500mm left at both ends of link slab. These 500mm exposed No.6 bars were lap spliced with new No.5 bars to simulate the retrofit of an existing bridge. A reinforcement ratio of 0.01, which is lower than that of specimen LS-1 and LS-2, was employed as the reinforcement ratio of the specimen LS-3.

3.3 Experimental test setup and procedure

The experimental investigation of ECC link slabs was conducted using a representative section (711mm wide) of a link slab between the inflection points of the adjacent deck slabs (3.25m long). The zero moment condition at the inflection points as well as the boundary conditions at the pier were simulated by roller supports at the specimen end supports and at the load points (Fig.5). For practical purposes, the test setup represents an inverted orientation of the link slab region.

The loading sequence chosen was similar to the procedure adapted by MDOT[4]. All specimens were subjected to sequential static loading up to two times the deflection causing a rebar stress in the specimen LS-1 of 40% of its yield strength, which is the current limit stress criterion for concrete link slab design. The final step of sequential static loading stage simulates potential overload. In the subsequent cyclic loading procedure, the load at 40% yield of the reinforcement in LS-1 is chosen as the mean load with an amplitude up to maximum deflection at 0.00375 rad. rotation angle. This maximum rotation angle θ_{max} (0.00375 rad.) corresponds to the allowable deflection of a bridge span under live load (Δ_{max}, $L_{sp}/800$ in AASHTO code).

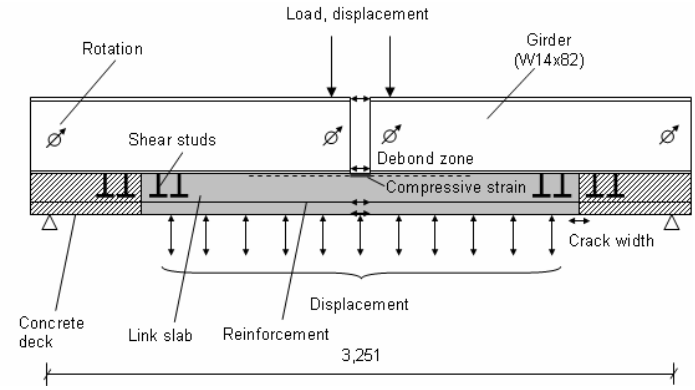

Fig.5 Laboratory test setup and instrumentation of specimen. (Dimensions are in mm)

$$\theta_{\max} = \frac{\Delta_{\max}}{\Delta}\theta = \frac{\Delta_{\max}}{PL_{sp}^3/48EI_{sp}}\frac{PL_{sp}^2}{16EI_{sp}} = \frac{L_{sp}}{800}\frac{3}{L_{sp}} = 0.00375\,rad. \quad (2)$$

where L_{sp} is bridge span length and EI_{sp} is flexural rigidity of the bridge section. Cyclic loading was carried out to 100,000 cycles. During testing, the applied load, displacements, rotation angles, strains at the compressive face of link slab at midspan and interfacial crack width of the specimen as indicated in Fig.5 are monitored using a data acquisition system. Cracks are marked and crack widths are measured at each loading sequence during the monotonic pre-loading procedure as well as at every 10,000 cycles during the cyclic loading procedure.

4. Results and Discussions

4.1 Fatigue cracking resistance of link slab specimens

The recorded data indicates that the stiffnesses of the specimens remained unchanged during the cyclic testing, i.e., there was no global damage observed (Fig.6). However, the structural stiffness of specimen LS-3 was measured to be lower than those of the other two specimens while specimen LS-1 and LS-2 had a similar stiffness. This is due to the relatively low reinforcement ratio of LS-3, which was deliberately chosen based on relatively low rebar stress in ECC link slabs compared to concrete link slab[6]. Realization of low structural stiffness will be an advantage of an ECC link slab since the structural effect on the main bridge span can be minimized when the link slab acts more like a hinge rather than a continuous element.

Although global damage did not occurr in all the specimens, the cracking patterns were distinctly different for the concrete and ECC link slabs. For LS-1, no additional cracks were seen and the existing cracks generated during the pre-loading stage gradually grew wider. The crack widths in concrete ultimately reached 635μm at 100,000 loading cycles (Fig.6). In contrast, additional microcracks appeared as the number of loading cycles increased in ECC link slab specimens (LS-2 and LS-3), while the existing crack

widths were maintained below 50μm, slightly opening and closing at the maximum and minimum loads, up to 100,000 cycles.

Fig.7 presents the comparison of the marked crack pattern between LS-1, LS-2, and LS-3. A large number of hairline cracks were observed in the ECC link slab specimens while a small number of large cracks in LS-1 specimen were observed. This demonstrates that fatigue cracking resistance of ECC link slabs, in terms of crack width, is independent of the reinforcement ratio because of the inherent multiple cracking and tight crack width control of ECC. Such reduced crack width and high ductility in ECC indicate the potential realization of macroscopically crack free concrete bridge deck systems through the use of ECC material in link slabs. It is also expected that the low permeability of ECC due to relatively small crack widths will enhance the durability of an ECC link slab particularly under severe environmental conditions, such as in regions where deicing salts are frequently used.

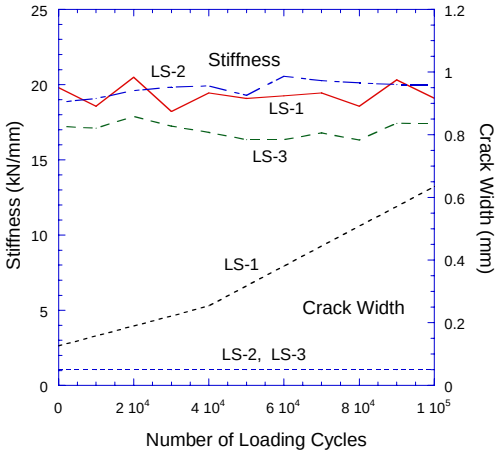

Fig.6 Stiffness change and crack width evolution of link slab specimens.

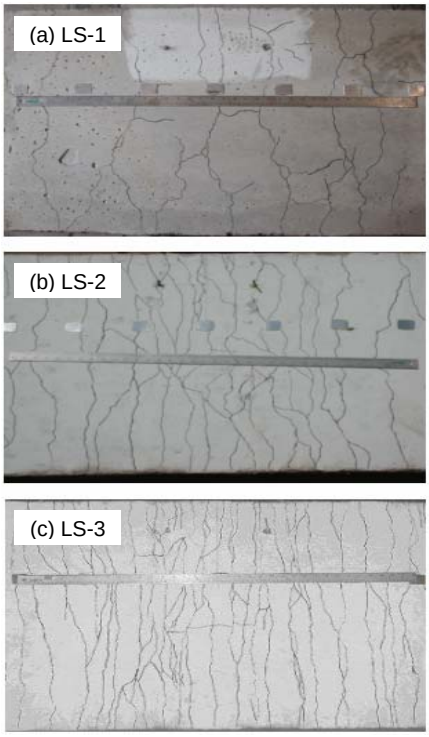

Fig.7 Crack pattern marked with magic ink pen after cyclic test

Besides the stress limitation requirement described above, the current design procedure of concrete link slab also requires limiting the maximum crack width at the top of the link slab. A minimum reinforcement ratio 0.015 has been suggeted with a clear cover

of 63mm for the purpose of controlling the crack width in the concrete link slab[7]. Therefore, the inherent tight crack width of ECC material is expected to provide a more efficient link slab design due to the decoupling of crack width and reinforcement ratio in addition to other advantages represented by enhanced durability and lower structural stiffness of ECC link slabs.

4.2 Fatigue cracking resistance at the concrete/ECC interface

There was no cracking observed at the interface between R/C deck slab and ECC link slab (Fig.8). In contrast, the cracking formed over the debond span of link slab up to the location of shear studs. This indicates that cracks should have appeared at the concrete/ECC interface if it had been located at the end of debond zone. The modification of the design to locate the concrete/ECC material interface away from the structural interface between the debond zone and girder/deck composite zone prevented cracking at the material interface. Furthermore, the additional shear studs placed between these two interfaces provided composite action between girder and ECC slab. As a result, concrete/ECC interface cracking caused by stress concentrations is prevented. Instead, cracking is limited to within the bulk part of ECC, where higher strength and sufficient strain capacity exist to accommodate the higher stress. This modification of the interface from conventional link slab design will provide enhanced integrity of concrete/ECC interface, preventing undesirable interfacial cracking.

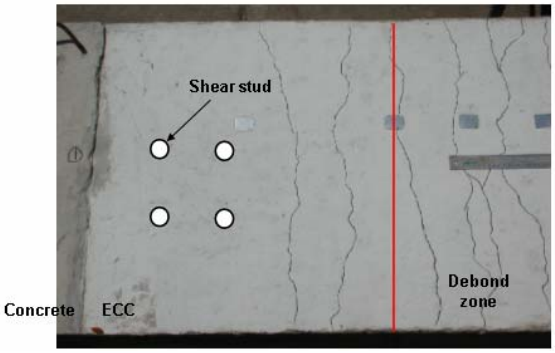

Fig.8 Crack pattern marked with magic ink pen at interface zone in LS-2 specimen

5. Conclusions

The following conclusions can be drawn from the current experimental results:

1. Property requirements of ECC material for link slabs were examined prior to material choice. It was revealed that the property requirements for link slab applications were satisfied with the hardened properties of ECC material chosen in the present study. This ECC exhibited strain-hardening behavior with tensile strain capacity of 3-5% accompanied by multiple cracking with crack widths of 40 μm. These properties more than satisfied the demand of tensile ductility and crack width control.

2. The cyclic tests performed on three link slabs revealed that the stiffnesses of the three specimens remained unchanged during cyclic testing. However, the crack widths of the concrete link slab (635μm) at 100,000 loading cycles were substantially larger than those of the ECC link slabs (<50μm), by one order of magnitude. The tight crack width of ECC under cyclic loading will positively contribute to the durability of an ECC link slab, and the potential realization of macroscopically crack free concrete deck systems as well.
3. In terms of crack width limitations, the use of ECC, with crack widths and spacing as inherent material properties, will decouple the dependency of crack width on the amount of rebar. This decoupling allows the simultaneous achievement of structural need (lower flexural stiffness of the link slab) and durability need (crack width control) of the link slab.
4. There was no cracking observed at the interface between ECC link slab and R/C deck slab during cyclic testing, while micro-cracking formed over the debond span of the link slab up to the shear studs, as intended. This is due to the fact that the modified location of concrete/ECC interface as well as the additional shear studs installed in ECC link slab, caused a shifting of the stress concentration from the concrete/ECC interface to the part of the ECC link slab. This modification is expected to provide enhanced integrity of the interface, preventing interfacial cracking.
5. Compared to R/C link slab, ECC link slab provides better structural performance via its lower stiffness (with lower reinforcement ratio needed), and better durability performance via its crack width control as an innate material property.

References

1. Caner, A. and Zia, P., “Behavior and Design of Link Slab for Jointless Bridge Decks,” PCI J., May-June, 1998, pp.68-80.
2. Wang, K., Jansen, D.C., and Shah, S., "Permeability study of cracked concrete," Cement and Concrete Research, Vol.27, No.3, 1997, pp. 381-393.
3. Li, V.C. et al., 1st Progress Report on Durable Link Slabs for Jointless Bridge Decks Based on Strain-Hardening Cementitious Composites, Michigan Department of Transportation, June, 2002.
4. Gilani, A., and Juntunen, D., Link Slabs for Simply Supported Bridges: Incorporating Engineered Cementitious Composites, Report No. MDOT SPR-54181, Michigan Department of Transportation, July, 2001.
5. Li, V.C., “Reflections on the Research and Development of Engineered Cementitious Composites (ECC),” Proceedings of the JCI International Workshop on Ductile Fiber Reinforced Cementitious Composites (DFRCC) - Application and Evaluation (DRFCC-2002), Takayama, Japan, Oct. 2002, pp.1-21.
6. Kim, Y.Y., Fischer, G. and Li, V.C., "Performance of Bridge Deck Link Slabs Designed with Ductile ECC," Submitted, ACI Journal, 2003.
7. Oesterle, R.G. et al., Jointless and Integral Abutment Bridges – Summary Report, Final Report to Federal Highway Administration, Washington D.C., 1999.